Monthly Notices of the ROYAL ASTRONOMICAL SOCIETY

MNRAS **480,** 1363–1371 (2018) doi:10.1093/mnras/sty1816

The recurrent nova RS Oph: simultaneous *B*- and *V*- band observations of the flickering variability

R. K. Zamanov,[1★] S. Boeva,[1] G. Y. Latev,[1] J. Martí,[2] D. Boneva,[3] B. Spassov,[1] Y. Nikolov,[1] M. F. Bode,[4] S. V. Tsvetkova[1] and K. A. Stoyanov[1]

[1] *Institute of Astronomy and National Astronomical Observatory, Bulgarian Academy of Sciences, 72 Tsarigradsko Shose, 1784 Sofia, Bulgaria*
[2] *.Departamento de Física (EPSJ), Universidad de Jaén, Campus Las Lagunillas, A3-420, 23071 Jaén, Spain*
[3] *Space Research and Technology Institute, Bulgarian Academy of Sciences, ul. Akad. G. Bonchev blok 1, 1113 Sofia, Bulgaria*
[4] *Office of the Vice Chancellor, Botswana International University of Science and Technology, Private Bag 16, Palapye, Botswana*

Accepted 2018 June 30. Received 2018 June 30; in original form 2018 March 7

ABSTRACT

We performed 48.6 hr (over 28 nights) of simultaneous *B*- and *V*- band observations of the flickering variability of the recurrent nova RS Oph in quiescence. During the time of our observations, the brightness of the system varied in the range $13.2 > B > 11.1$ and the colour in the range $0.86 < B - V < 1.33$. We find that RS Oph becomes bluer as it becomes brighter; however, the hot component becomes redder as it becomes brighter (assuming that the red giant is non-variable). During all the runs, RS Oph exhibits flickering with amplitude 0.16–0.59 mag in the *B* band. We find that the flickering source has colour $-0.14 < B - V < 0.40$, temperature in the range $7200 < T_{\rm fl} < 18\,900$ K, and an average radius $1.1 < R_{\rm fl} < 6.7$ $R_{\odot}$. We do not find a correlation between the temperature of the flickering and the brightness. However, we do find a strong correlation (correlation coefficient 0.81, significance 1.1×10^{-7}) between the *B*-band magnitude and the average radius of the flickering source; that is, as the brightness of the system increases, the size of the flickering source also increases. The estimated temperature is similar to that of the bright spot of cataclysmic variables. The persistent presence of flickering indicates that the white dwarf is actively accreting material for the next outburst.

Key words: accretion, accretion discs – binaries: symbiotic – stars: individual: RS Oph – novae, cataclysmic variables.

1 INTRODUCTION

RS Oph (HD 162214) is a symbiotic recurrent nova that exhibits recurrent nova outbursts approximately every 15–20 yr. During the outbursts, the brightness rises from an initial value of $V \sim 11$ to V ˜ 6 mag. Most likely, the recurrent nova outbursts are the result of a thermonuclear runaway on the surface of the white dwarf (Starrfield 2008); however, some authors suggest that there is a dwarf nova-like accretion disc instability (King & Pringle 2009; Alexander et al. 2011).

RS Oph contains an M giant mass donor (Dobrzycka & Kenyon 1994; Anupama & Mikołajewska 1999) and a massive (1.2–1.4 $M_{\odot}$) carbon–oxygen white dwarf (Mikołajewska & Shara 2017). The mass transfer mechanism could be via Roche lobe overflow or stellar wind capture, and is still the subject of debate (Somero, Hakala & Wynn 2017). Booth, Mohamed & Podsiadlowski (2016) found that the quiescent mass transfer produces a dense outflow, concentrated towards the binary orbital plane, and that an accretion disc forms around the white dwarf. Furthermore, a photoionization model of the quiescent spectrum indicates the presence of a low-luminosity accretion disc (Mondal et al. 2018).

Brandi et al. (2009) found that the orbital period of the system is 453.6 d and gave a mass ratio $q = M_{\rm RG}/M_{\rm WD} = 0.59 \pm 0.05$, which corresponds to a mass of the red giant of $M_{\rm RG}$=0.68–0.80 $M_{\odot}$ and an inclination of the orbit of $i = 49^{\circ}-52^{\circ}$. The orbit of the system is consistent with its being circular with a period of 455.7 d (Fekel et al. 2000).

The most recent nova outburst of RS Oph occurred on 2006 February 12 (Narumi et al. 2006; Evans et al. 2008), and the multiwavelength observations extended our knowledge of the mechanisms and physics of nova explosions and of the formation of planetary nebulae. The optical and radio observations after the outburst confirmed an asymmetric double-ring structure of the nova remnant (O'Brien et al. 2006; Bode et al. 2007; Rupen, Mioduszewski & Sokoloski 2008). The X-ray observations show that the nova interacts with the dense circumstellar medium, leading to a deceleration of the material (Sokoloski et al. 2006; Bode et al. 2006). The ejecta have low mass, namely $M_{\rm ej} \sim 10^{-7}$–10^{-6} $M_{\odot}$, and high velocity,

★ E-mail: rkz@astro.bas.bg

namely $\upsilon_{ej} \gtrsim 4000\,\mathrm{km\,s^{-1}}$ (Bode et al. 2006; Sokoloski et al. 2006; Vaytet et al. 2011).

The flickering is seemingly irregular, with light variations on time-scales of a few minutes with amplitude of a few times 0.1 mag. The flickering of RS Oph has been observed by Walker (1977), Bruch (1980), Gromadzki et al. (2006) and others. The study of flickering in any interacting binary system is important because it allows us to probe what is happening in the inner regions of the accretion disc. The release of luminosity here follows variations at larger accretion disc radii on time-scales of the order of, or larger than, the local viscous time-scale. The variations are expected to be of flicker-noise-type according to the α-based accretion disc models pioneered by Lyubarskii (1997). Improving our knowledge of flickering in RS Oph enables us to widen our exploration of the parameter space of accretion discs around mildly compact objects such as its white dwarf companion. In this context, our RS Oph observations contribute to a complementary view of flickering sources beyond previous studies, which have focused on black holes in X-ray binary and active galactic nuclei systems. With its unusual flickering properties among symbiotic stars, RS Oph provides an excellent alternative workbench for theorists to test their accretion disc models, and to gain an understanding of phenomena such as the widely observed rms–flux relationship (see Scaringi et al. 2012).

Here, we report quasi-simultaneous observations of the flickering variability of the recurrent nova RS Oph in two optical bands, namely *B* and *V*, and analyse the colour changes, temperature and radius of the flickering source and their response to the brightness variations.

2 OBSERVATIONS

The observations were performed with five telescopes equipped with CCD cameras:

(i) the 2.0-m telescope of the National Astronomical Observatory (NAO) Rozhen, Bulgaria (Bonev & Dimitrov 2010);
(ii) the 50/70-cm Schmidt telescope of NAO Rozhen;
(iii) the 60-cm telescope of NAO Rozhen (Popov & Dimitrov 2011);
(iv) the 60-cm telescope of the Belogradchik Observatory, Bulgaria (Strigachev & Bachev 2011);
(v) the 41-cm telescope of the University of Jaén, Spain (Martí, Luque-Escamilla, & García-Hernández 2017).

The data reduction was carried out using IRAF (Tody 1993) following standard recipes for the processing of CCD images and aperture photometry. A few comparison stars from the list of Henden & Munari (2006) were used. Fig.1 provides two examples of our data – the observed variability in the *B* and *V* bands is plotted together with the calculated *B* – *V* colour. The typical photometric errors are 0.006 mag in the *B* band and 0.005 mag in the *V* band.

We have 28 nights with simultaneous observations in *B* and *V* bands during the period 2008 July– 2017 September. The $B - V$ colour is calculated for 2749 points in total. During our observations, the brightness of RS Oph was in the following ranges:

$11.121 \le B \le 13.208$,
$10.093 \le V \le 11.908$,
$0.864 \le B - V \le 1.333$,

with mean B=12.204, mean V=11.106, mean $B-V$=1.098. The peak-to-peak amplitude of the flickering in the *B* band is in the range 0.16–0.59 mag.

The journal of observations is given in Table 1. The table provides the following information: the date (in format YYYYMMDD), the band, the telescope, the number of data points over which the *B* – *V* colour is calculated, the average, minimum and maximum magnitudes in the corresponding band, the dereddened colour of the flickering source $(B - V)_{01}$ and $(B - V)_{02}$, T_1 and T_2 (temperature of the flickering source), R_{fl} and R_2 (radius of the flickering source). More details of how we calculated these parameters and the denoted symbols are given in Section 5.

3 INTERSTELLAR EXTINCTION AND RED GIANT CONTRIBUTION

3.1 Interstellar reddening

We have nine high-resolution spectra obtained with the FEROS spectrograph attached to the 2.2-m telescope ESO La Silla and with the echelle spectrograph ESPERO at the 2.0-m telescope of NAO Rozhen. We compared these spectra with spectra of a few red giants with similar spectral type and measured the equivalent widths of four interstellar features clearly visible in the high-resolution spectra. Using the equivalent width of KIλ7699 and the calibration by Munari & Zwitter (1997), we found $0.60 < E(B - V) < 0.83$. Using the diffuse interstellar bands (DIBs) and results of Puspitarini, Lallement & Chen (2013), we derived for DIB λ6613 $0.59 < E(B - V) < 0.80$, for DIB λ5780 $0.57 < E(B - V) < 0.69$, and for DIB λ5797 $0.65 < E(B - V) < 0.78$. Taking into account the individual errors, we estimate $E(B - V) = 0.69 \pm 0.07$. This is in agreement with (i) the value $E(B - V) = 0.73 \pm 0.10$ given in Snijders (1987) on the basis of UV spectra and (ii) the Galactic dust reddening for a line of sight to RS Oph (NASA/IPAC IRSA: Galactic Reddening and Extinction Calculator), $0.59 \le E(B - V) \le 0.69$, which should be considered as an upper limit for the interstellar reddening. Hereafter we use $E(B - V) = 0.69 \pm 0.07$.

3.2 Parameters of the red giant in RS Oph

On the basis of the light curves of RS Oph after the 2006 outburst (see section 3 in Zamanov et al. 2015), we estimated that the brightness of the red giant is $m_V \approx 12.26$. To check this value, we assumed that the ratio between the variable and non-variable parts of the hot-component contribution to the brightness is equal in the *U* and *V* bands. The flickering of RS Oph is clearly visible in all *UBVRI* bands, with amplitude increasing towards the blue. Using data from Zamanov et al. (2010, 2015), we estimated the magnitude of the red giant in the *V* band to be $m_V = 12.19 \pm 0.10$. This value (although based on an assumption) is in agreement with $m_V \approx 12.26$ above.

Shenavrin, Taranova & Nadzhip (2011) found the spectral type of the red giant to be M2pe from IR photometry. Mondal et al. (2018) derived the spectral type to be M2-M3 from the absorption-band indices. Skopal (2015a) found that the radiation from the giant corresponds to an effective temperature of $T_{\rm eff} = 3800-4000$K and a radius of $R_g = (61-55)(d/1.6\,{\rm kpc})\,{\rm R_\odot}$. Comparing our spectra with spectra of red giants (Houdashelt et al. 2000; Bagnulo et al. 2003; Zhong et al. 2015), we estimate a similar spectral type, M2III. In Fig. 2 we plot one of our spectra of RS Oph. The spectrum is corrected for the interstellar extinction using $E(B–V)$=0.69, the contribution of the hot continuum is subtracted, and the spectrum is normalized at 8350 Å. The emission lines are not removed. We compared the spectrum with templates of M giants by Zhong et al. (2015). The red line is the template spectrum of an M2III giant from Zhong et al. (2015), for which we achieved the best agreement.

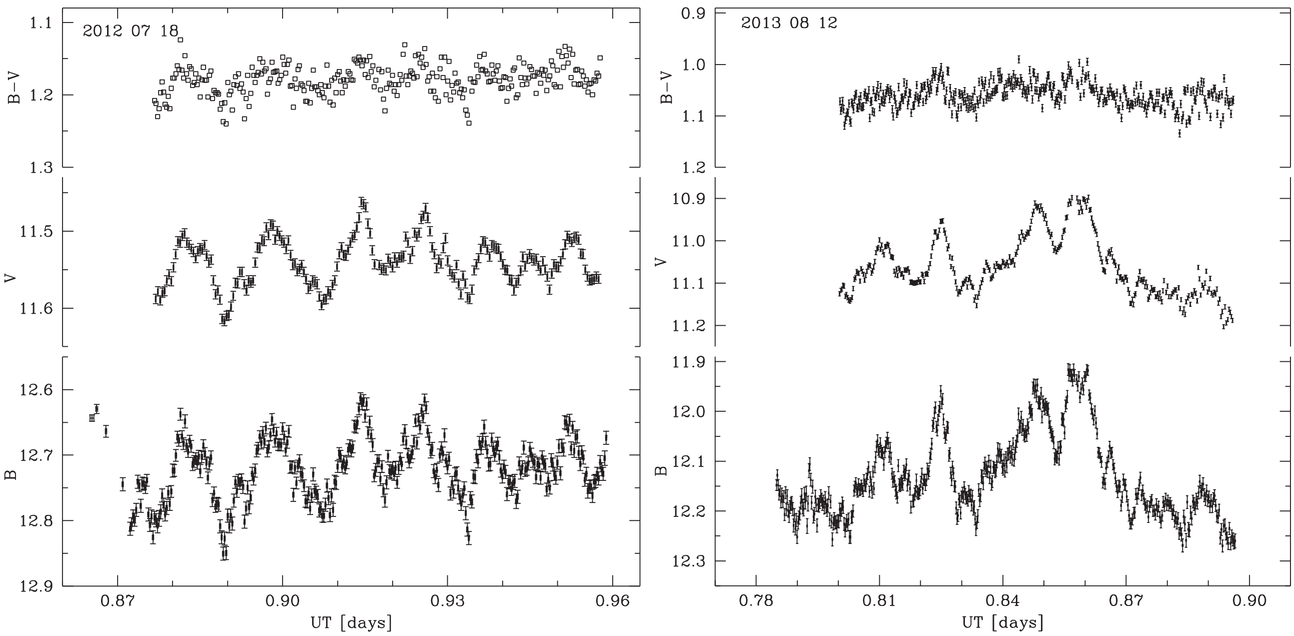

Figure 1. Example of our observations: light curves of RS Oph in the *B* and *V* bands together with the calculated *B* –*V* colour.

An M2III star is expected to have an effective temperature of 3695–3750K and a radius of 57.8–60.5 $R_\odot$ (van Belle et al. 1999). For such a giant and solar metallicity model, Houdashelt et al. (2000) give $T_{\rm eff} = 3740$ K, $\log g = 0.81$, $B - V = 1.629$, $V - I = 1.927$. We adopt for the brightness of the red giant in the optical bands $m_B = 14.660$ and $m_V = 12.261$. The typical 1σ error of these magnitudes is about ±0.05 mag.

4 VARIABILITY IN THE *B* AND *V* BANDS

In Fig. 3 we plot the *B*- versus *V*-band magnitude. The left panel (Fig. 3a) gives the observed magnitudes of RS Oph. The right panel (Fig. 3b) shows the dereddened magnitudes of the hot component (i.e. the red giant contribution is subtracted using the magnitudes given in Section 3.2).

4.1 *B* –*V* colour

In Fig. 4, we plot colour–magnitude diagrams. The colour–magnitude diagram is quite different from that of the cataclysmic variable AE Aqr (Zamanov et al. 2017). In the case of AE Aqr, all the data occupy a well-defined strip on the colour-magnitude diagram (see fig. 3 of Zamanov et al. 2017). For RS Oph, such a strip is not visible regarding all data, although the observations from each night are placed on a strip on the diagram. This indicates that the flickering behaviour in the case RS Oph is more complicated and/or has a different mechanism

In Fig. 5, we plot the calculated mean values for each night (one night – one point). The error bars correspond to the standard deviation of the run. It is seen that the system becomes bluer as it becomes brighter; however, the hot component becomes redder as it becomes brighter. There is a correlation between the mean colour and magnitude of the hot component. The Pearson correlation coefficient is 0.70, Spearman's (rho) rank correlation is 0.69, and the statistical significance *p*-value is 5.5×10^{-5}. This indicates that the hot component becomes redder as it becomes brighter.

5 FLICKERING LIGHT SOURCE

In his remarkable paper, Bruch (1992) proposed that the light curve of a white dwarf with flickering can be separated into two parts – constant light and a variable (flickering) source. Following his assumptions, we calculated the flux of the flickering light source as $F_{\rm fl1} = F_{\rm av} - F_{\rm min}$, where $F_{\rm av}$ is the average flux during the run and $F_{\rm min}$ is the minimum flux during the run (corrected for the typical error of the observations). An extension of the method was proposed by Nelson et al. (2011), who suggested using $F_{\rm fl2} = F_{\rm max} - F_{\rm min}$, where $F_{\rm max}$ is the maximum flux during the run. $F_{\rm fl1}$ and $F_{\rm fl2}$ are the fluxes of the flickering calculated following Bruch (1992) and Nelson et al. (2011) respectively.

Essentiallly, the method of Bruch (1992) refers to the average luminosity of the flickering source, while that of Nelson et al. (2011) refers to its maximal luminosity. We calculated $F_{\rm fl1}$ and $F_{\rm fl2}$ for each band, using the values given in Table 1 and the calibration for a zero-magnitude star $F_0(B) = 6.293 \times 10^{-9}$ erg cm^{-2} s^{-1} Å^{-1}, $\lambda_{\rm eff}(B) =$ 4378.12 Å, $F_0(V) = 3.575 \times 10^{-9}$ erg cm^{-2} s^{-1} Å^{-1} and $\lambda_{\rm eff}(V)$ = 5466.11 Å, as given by the Spanish virtual observatory Filter Profile Service (Rodrigo et al. 2018, see also Bessel 1979). It is worth noting that while the calculated colours of the hot component depend on the assumed red giant brightness, the parameters of the flickering source are independent of the red giant parameters.

Using the method of Bruch (1992), we find that in the *B* band the flickering light source contributes about 13 per cent of the average flux of the system, with $0.06 \le F_{\rm fl1}/F_{\rm av} \le 0.24$. In the *V* band, its average contribution is 11 per cent, with $0.05 \le F_{\rm fl1}/F_{\rm av} \le 0.19$. Using the method of Nelson et al (2011), we find that in the *B* band the flickering light source contributes about 25 per cent of the maximal flux of the system, with $0.13 \le F_{\rm fl2}/F_{\rm max} \le 0.42$. In the *V* band, its contribution is about 21 per cent, with $0.10 \le F_{\rm fl2}/F_{\rm max} \le$ 0.36.

From the amplitude–flux relationship (rms–flux relationship), we expect that the luminosity of the flickering source will increase as the brightness increases. However, it is not clear a priori which parameter – temperature or radius (or both) – increases.

Table 1. Simultaneous CCD observations of RS Oph in the *B* and *V* bands and the calculated parameters of the flickering source. $(B-V)_{01}$, T_1 and $R_{\rm fl}$ are the dereddened colour, temperature and radius of the flickering source calculated following Bruch (1992); $(B-V)_{02}$, T_2 and R_2 are those following Nelson et al. (2011) – see Section 5.

Date	Band	Telescope	N_{B-V}	Average Min Max [mag] [mag] [mag]	$(B-V)_{01}$	T_1 [K]	$R_{\rm fl}$ [$R_\odot$]	$(B-V)_{02}$	T_2 [K]	R_2 [$R_\odot$]
20080706	*B*	70-cm Sch[1]	49	12.4711 12.380 12.615	0.1117	10515	2.322	0.1189	10384	3.096
	V	2.0-m Roz[2]		11.2308 11.168 11.325						
20090615	*B*	60-cm Roz[3]	76	11.7666 11.597 11.951	0.1442	9948	3.954	0.2118	9102	6.686
	V	60-cm Bel[4]		10.7420 10.581 10.895						
20090721	*B*	60-cm Roz	57	12.0280 11.876 12.277	0.2302	8872	4.937	0.1083	10576	4.773
	V	60-cm Bel		10.9963 10.891 11.219						
20090723	*B*	70-cm Sch	38	11.9789 11.857 12.099	0.2025	9219	3.360	0.1927	9341	4.793
	V	2.0-m Roz		10.9740 10.865 11.082						
20100430	*B*	60-cm Roz	62	11.7409 11.603 11.848	0.3043	7964	4.732	0.1754	9558	5.199
	V	60-cm Roz		10.6227 10.521 10.718						
20100501	*B*	60-cm Roz	66	11.4349 11.121 11.612	0.2539	8576	5.936	0.2554	8558	10.7083
	V	60-cm Roz		10.3817 10.093 10.541						
20120427	*B*	60-cm Roz	58	12.1117 11.934 12.271	0.3551	7541	5.408	0.1868	9415	5.271
	V	60-cm Bel		10.9899 10.863 11.138						
20120613	*B*	60-cm Roz	33	12.5301 12.380 12.671	0.2671	8411	3.349	0.1345	10100	3.564
	V	60-cm Roz		11.3755 11.274 11.492						
20120718	*B*	70-cm Sch	200	12.7207 12.617 12.850	-0.0493	14379	1.254	0.0573	11504	2.351
	V	2.0-m Roz		11.5400 11.462 11.617						
20120721	*B*	60-cm Bel	199	12.4126 12.201 12.552	-0.1415	18972	1.086	-0.1561	19783	1.736
	V	60-cm Bel		11.4321 11.288 11.524						
20120815	*B*	60-cm Roz	63	12.9043 12.618 13.208	0.2897	8129	4.277	0.2549	8564	5.761
	V	70-cm Sch		11.6736 11.452 11.908						
20120816	*B*	2.0-m Roz	185	12.7805 12.666 12.897	0.0039	12783	1.358	0.1430	9962	2.887
	V	70-cm Sch		11.5624 11.472 11.633						
20130702	*B*	60-cm Roz	46	12.1955 11.982 12.368	0.0455	11718	2.422	-0.1098	17211	2.321
	V	60-cm Roz		11.1140 10.988 11.237						
20130710	*B*	70-cm Sch	127	12.0329 11.887 12.207	0.1903	9371	3.784	0.2375	8781	5.997
	V	70-cm Sch		11.0399 10.896 11.196						
20130812	*B*	70-cm Sch	335	12.1202 11.916 12.270	0.3177	7852	4.796	0.1906	9368	5.476
	V	2.0-m Roz		11.0603 10.897 11.203						
20130813	*B*	70-cm Sch+60-cm Roz	91	12.5788 12.476 12.659	0.1228	10313	1.728	-0.0084	13152	1.855
	V	2.0-m Roz		11.4438 11.381 11.503						
20130906	*B*	60-cm Bel	39	12.0118 11.848 12.152	0.2258	8928	3.779	0.2608	8490	6.376
	V	60-cm Bel		10.8648 10.723 10.977						
20140621	*B*	60-cm Bel	65	12.5414 12.459 12.614	0.2318	8852	2.199	0.1190	10382	2.469
	V	60-cm Bel		11.4264 11.369 11.487						
20140622	*B*	60-cm Bel	104	12.6152 12.347 12.864	0.1780	9525	3.305	0.2928	8090	6.958
	V	60-cm Bel		11.5765 11.303 11.786						
20140729	*B*	70-cm Sch	32	12.3089 12.228 12.430	0.2826	8218	3.619	0.3866	7278	6.191
	V	70-cm Sch		11.2557 11.163 11.368						
20140831	*B*	70-cm Sch	54	12.0877 11.950 12.303	0.1218	10331	3.434	0.1073	10595	4.361
	V	70-cm Sch		10.9762 10.873 11.136						
20160726	*B*	70-cm Sch	63	12.3041 12.151 12.471	0.2016	9230	3.367	0.2142	9072	4.993
	V	2.0-m Roz		11.0561 10.941 11.174						
20160728	*B*	70-cm Sch	92	12.2771 12.084 12.455	0.1039	10656	2.742	0.1855	9431	5.107
	V	70-cm Sch		11.0810 10.926 11.201						
20170329	*B*	70-cm Sch	116	12.0432 11.925 12.219	0.2167	9041	4.041	0.2650	8438	6.140
	V	70-cm Sch		10.7978 10.701 10.924						
20170528	*B*	60-cm Bel	88	12.1335 11.960 12.252	0.0558	11531	2.142	0.0264	12108	3.259
	V	60-cm Bel		11.1661 11.028 11.262						
20170626	*B*	60-cm Bel	144	11.6834 11.557 11.814	0.3965	7196	6.672	0.3649	7459	8.890
	V	60-cm Bel		10.5115 10.400 10.632						
20170719	*B*	41-cm Jaén[5]	133	11.7123 11.551 11.895	0.1709	9614	4.284	0.0747	11187	4.755
	V	41-cm Jaén		10.7409 10.617 10.905						
20170904	*B*	41-cm Jaén	65	11.6785 11.557 11.805	0.3347	7711	5.645	0.1013	10704	4.409
	V	41-cm Jaén		10.6443 10.567 10.770						

[1]the 50/70-cm Schmidt telescope of NAO Rozhen
[2]the 2.0-m telescope of NAO Rozhen
[3]the 60-cm telescope of NAO Rozhen
[4]the 60-cm telescope of the Belogradchik Observatory
[5]the 41-cm telescope of the University of Jaén

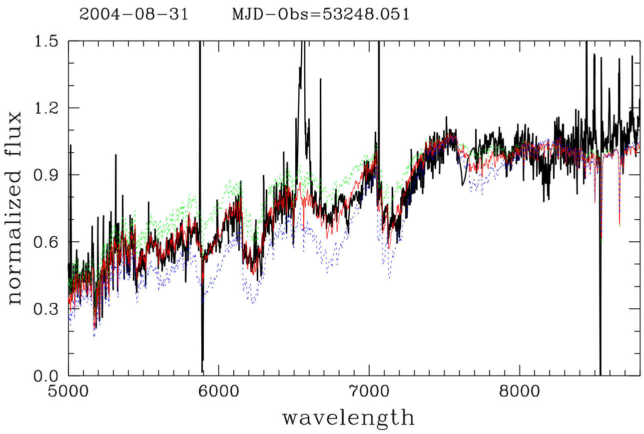

Figure 2. The spectrum of RS Oph is denoted by the black line. The spectrum is corrected for interstellar extinction using $E(B–V)$=0.69, and the contribution of the hot continuum is subtracted. The green, red and blue lines are template spectra of M1III, M2III and M3III giants, respectively, from Zhong et al. (2015).

5.1 *B –V* colour and temperature of the flickering source

The calculated de-reddened colours of the flickering light source are given in Table 1, where $(B-V)_{01}$ is calculated using $F_{\rm av}$ and $F_{\rm min}$, while $(B-V)_{02}$ is calculated using $F_{\rm max}$ and $F_{\rm min}$ (the subscript 0 means dereddened colour). The typical error is ±0.05 mag.

In Fig. 6, we plot $(B-V)_{02}$ versus $(B-V)_{01}$. The solid line represents $(B-V)_{02}=(B-V)_{01}$. To check for a systematic shift between the two methods, we performed a linear least-squares approximation in one dimension ($y=a+bx$), when both x and y data have errors. We obtained $a=0.027\pm0.017$ and $b=1.007\pm0.093$. A Kolmogorov–Smirnov test gives a Kolmogorov–Smirnov statistic of 0.18 and a significance level of 0.72. This means that the two methods give similar results and there is no systematic shift.

The average difference between $(B-V)_{01}$ and $(B-V)_{02}$ is ˜0.08 mag, which is comparable with the accuracy of our estimations. In Fig. 7, we plot $(B-V)_0$ versus the average B-band magnitude. We do not detect a correlation between the colour of the flickering source and brightness.

5.2 Temperature of the flickering source

We calculated the temperature of the flickering source using its dereddened colours and the colours of the black body (Straižys, Sudžius & Kuriliene 1976). T_1 was calculated using $(B-V)_{01}$, and T_2 was calculated using $(B-V)_{02}$. The values are given in Table 1. The two methods give similar results for the temperature of the flickering source as well as for $(B-V)_0$. The average values are T_1 = 9835 ± 2400 K and T_2 = 10 306± 2693 K. The slightly larger scatter of the values calculated following Nelson et al. (2011) is due to the fact that $F_{\rm av}$ is calculated more precisely than $F_{\rm max}$.

5.3 Radius of the flickering source

The radius of the flickering source $R_{\rm fl}$ was calculated using the derived temperature T_1 (Section 5.2), the B-band magnitude and assuming that the source is spherically symmetric. We obtained $0.92 < R_{\rm fl} < 5.6\ R_\odot$.

In Fig. 8 we plot $R_{\rm fl}$ versus the average B-band magnitude. It can be seen that $R_{\rm fl}$ increases when the brightness of the system increases. When we use all 28 points we find a moderate to strong correlation, with a Pearson correlation coefficient of 0.70, Spearman's (rho) rank correlation equal to 0.73, and the statistical significance p-value $\approx 9\times10^{-6}$.

The most deviant point is the run on 2012 August 15, the same run that deviates from the rms–flux relationship (see section 6.1 in Zamanov et al. 2015). When we remove this deviating point (owing to the low brightness and high-amplitude variability, i.e. number of points $N_{\rm pts}$ = 27), we obtained a strong and highly significant correlation between the radius of the flickering source and the average B-band magnitude of the hot component, with a Pearson correlation coefficient of 0.81, a Spearman's (rho) rank correlation of 0.83, and the statistical significance of the correlation p-value $\approx 1.1\times10^{-7}$.

We do not detect a significant correlation between the brightness and the radius of the flickering source calculated with $F_{\rm max}$.

5.4 Luminosity of the flickering source

The luminosity of the flickering source $L_{\rm fl}$ was calculated using the derived temperature and radius given in Table 1 and assuming that the source is spherically symmetric: $L_{\rm fl}=4\pi R_{\rm fl}^2\sigma T_1^4$, where σ is the Stefan–Boltzmann constant. We obtained 27 $L_\odot < L_{\rm fl} <$ 173 $L_\odot$.

6 DISCUSSION

Flickering variability is typical for accreting white dwarfs in cataclysmic variables and is considered an observational proof of accretion onto a white dwarf (Sokoloski & Bildsten 2010). It is a relatively rare phenomenon for symbiotic stars. Among more than 200 symbiotic stars known in our Galaxy, flickering is observed in only 11 objects. The last two were detected recently: V648 Car (Angeloni et al. 2013) and EF Aql (Zamanov et al. 2017). The flickering of RS Oph disappeared after the 2006 outburst (Zamanov et al. 2006), reappeared by day 241 of the outburst (Worters et al. 2007), and is visible in all our observations obtained from then until now. This indicates that the white dwarf is accumulating material for the next outburst.

Outbursts of RS Oph were recorded in 1898, 1933, 1958, 1967, 1985 and most recently in 2006 (Evans et al., 2008; Narumi et al. 2006). According to Schaefer (2010), two outbursts in 1907 and 1945 were missed when RS Oph was aligned with the Sun. The time interval between two consecutive outbursts is between 8.6 and 26.6 yr (Schaefer 2010; Adamakis et al. 2011). The last one took place in 2006, which means that the next one can be expected between the time of writing and 2032. We are now well into the observed historic inter-outburst period and we should be alert for the next eruption.

Changes in the emission from the Hα line are detected on timescales as short as 2 min (Worters & Rushton 2014). This time-scale is similar to that of the flickering variability and indicates that the flickering is partly re-processed in the nebula. The variability observed in Hα could be caused by changes in the photoionization of the nebula linked to the flickering activity. Given the discussion in section 6.2 of Sokoloski, Bildsten & Ho (2001) about the difficulty of producing rapid variability from the nebular emission, we expect the rapidly variable component of RS Oph to reflect the physical origin of the variations, for example in the accretion disc (or boundary layer, or hot spot), and not to be dominated by nebular features.

In the following paragraphs we discuss the implication of our results for three possible sites of origin of the flickering – the hot spot (e.g. Smak 1971), structures in the accretion disc (e.g. Baptista,

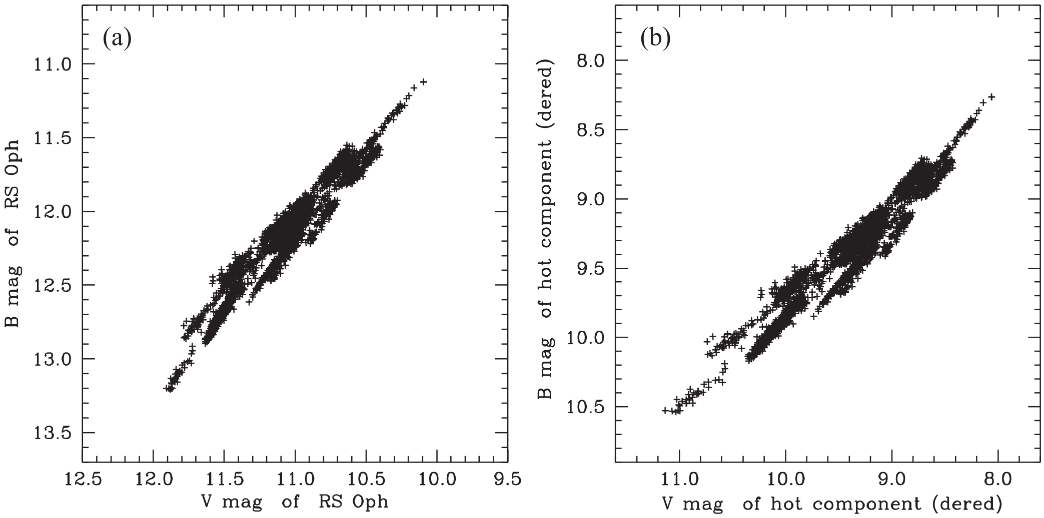

Figure 3. *B*- versus *V*- band magnitude: (a) observed, (b) calculated for the hot component.

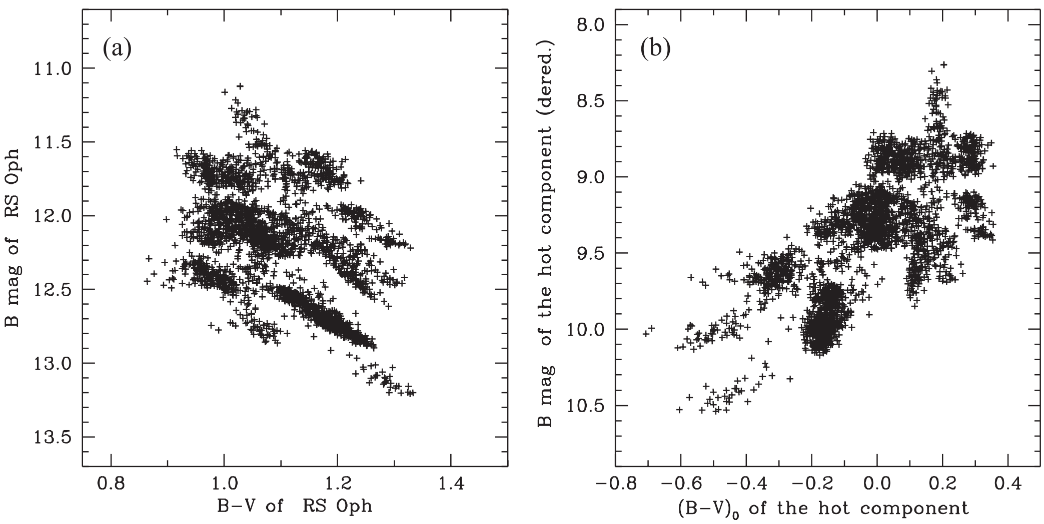

Figure 4. Colour–magnitude diagram: (a) observed, (b) calculated for the hot component.

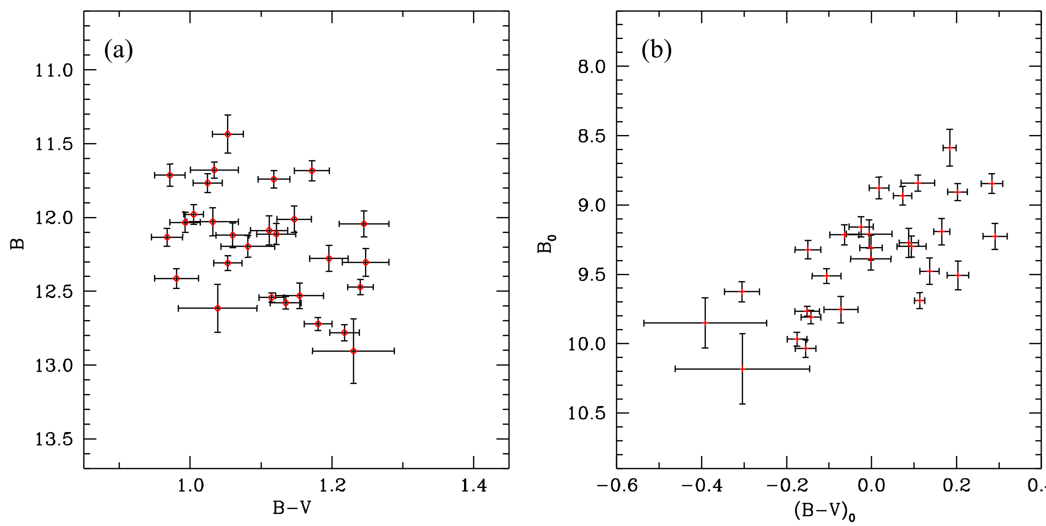

Figure 5. Mean colour–magnitude diagram, in which each point represent one run: (a) observed, (b) calculated for the hot component.

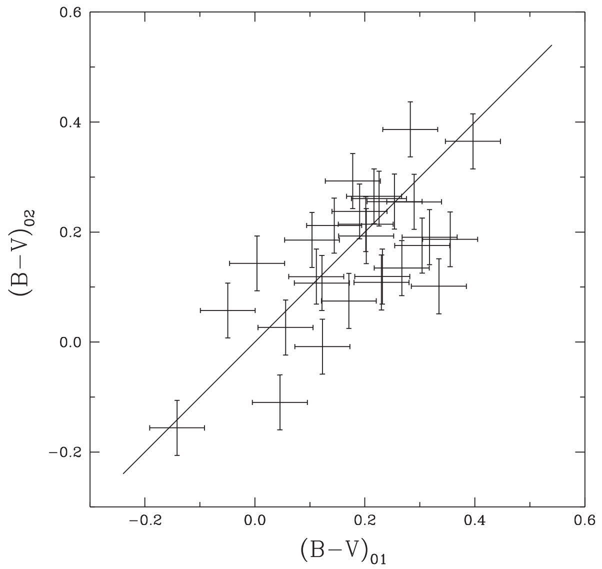

Figure 6. $(B-V)_{02}$ versus $(B-V)_{01}$: there is no systematic shift between the two methods. See text for details.

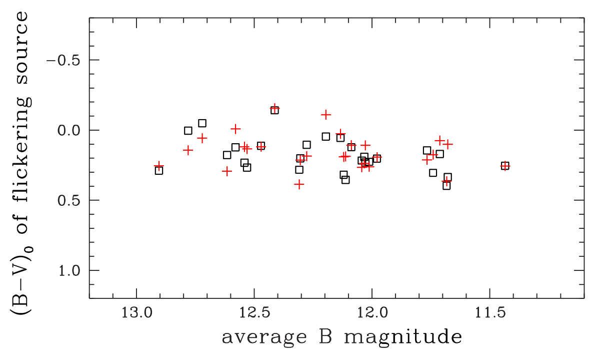

Figure 7. $(B-V)_0$ colour of the flickering source versus the average B magnitude. The squares represent $(B-V)_{01}$ calculated by method of Bruch (1992); the plus signs represent $(B-V)_{02}$ derived following Nelson et al. (2011). There is no tendency for the flickering source to become redder or bluer when the brightness changes.

Borges & Oliveira 2016) and the boundary layer (e.g. Bruch & Duschl 1993).

6.1 Typical time of the flickering

The wavelet analysis of the flickering of RS Oph performed by Kundra, Hric & Gális (2010) and Kundra & Hric (2014) found two sources of flickering: the first one with an amplitude of 0.1 mag and a frequency of 60–100 cycles per day, and the second one with an amplitude of 0.6 mag and a frequency lower than 60 cycles per day (with both parameters varying from night to night). Similar frequencies (17–144 cycles per day) are also visible in our data (Georgiev et al. 2018). Simon, Hudec & Hroch (2004), using observations with the Optical Monitoring Camera onboard the *INTEGRAL* satellite, found that the typical frequency was 30–50 cycles per day (i.e. a period of 48–29min) during the observations in 2003. Semiregular oscillations with a period of 82 ± 2 min on one night (about 17 cycles per day) have been detected by Dobrzycka, Kenyon & Milone (1996).

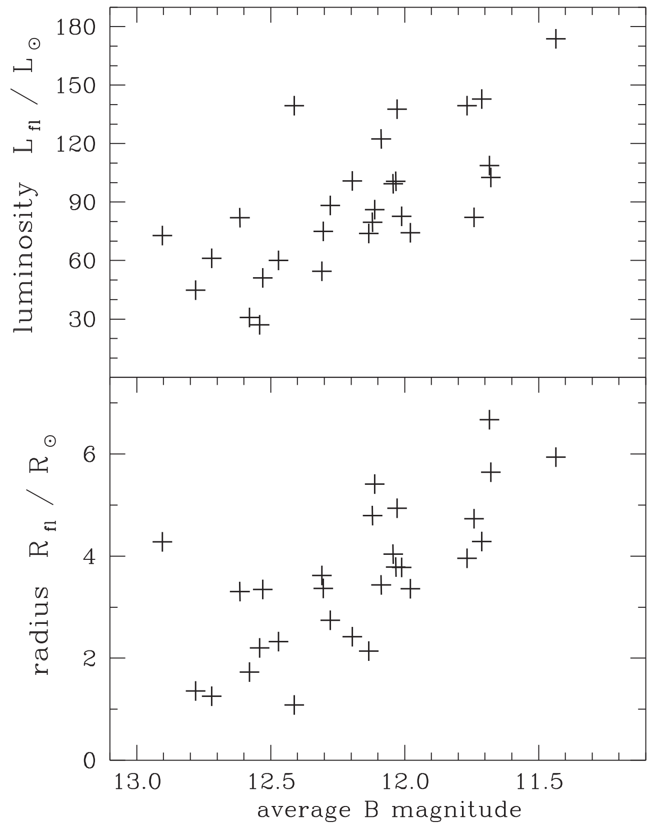

Figure 8. Luminosity and radius of the flickering source versus the average B- band magnitude. There is a well-defined tendency for the flickering source to become brighter and bigger when the brightness of the system increases.

Let us suppose that these quasi-periods correspond to the Keplerian period in the accretion disc around the white dwarf:

$$R_{\rm Kepl} = \left(\frac{G M_{\rm WD}}{4\pi^2 \nu^2} \right)^{1/3}, \quad (1)$$

where G is the gravitational constant, $R_{\rm Kepl}$ is the distance from the white dwarf, and ν is the frequency of the variability. For a 1.4 $M_{\odot}$ white dwarf, the frequencies correspond to $R_{\rm Kepl} \approx 0.2-0.5$ $R_{\odot}$. These values are 5–10 times smaller than the average radius of the flickering source calculated in Section 5.3. However they are similar to the radii estimated in Section 6.3.

6.2 Bright spot

The temperature and the size of the bright spot have been derived for a few cataclysmic variables. Wood et al (1989) calculated a temperature in the range 8600–15 000K for OY Car; Zhang & Robinson (1987) give $T = 11\,600 \pm 500$ K for U Gem; Robinson, Nather & Patterson (1978) give $T = 16\,000$ K for the bright spot in WZ Sge. For IP Peg three estimates exist: Marsh (1988) gives $T = 12\,000 \pm 1000$ K, Ribeiro et al. (2007) give 6000–10 000K, and Copperwheat et al. (2010) give 7000–13 000 K. The temperature of the optical flickering source of RS Oph is in the range $7000 < T_{\rm fl} < 18\,000$ K (see Section 4.1), which is similar to the temperature of the bright spot for the cataclysmic variables.

A bright spot is produced by the impact of the stream on the outer parts of the accretion disc. In the case of Roche-lobe overflow, this stream comes from the inner Lagrangian point L_1. If the red giant in RS Oph does not fill its Roche lobe, the white dwarf accretes material from its wind. In this case, an accretion cone and accretion wake will be formed [see fig. 1 of Jackson (1975) or fig. 4 of Ahmad, Chapman & Kondo (1983)]. The stream formed in the accretion wake should be similar to that formed from Roche-lobe overflow.

The luminosity of the bright spot is approximately (Shu 1976; Elsworth & James 1982)

$$L_{\rm bs} \approx \frac{1}{2} \upsilon_{\perp}^2 \dot{M}_{\rm acc}, \quad (2)$$

where $\dot{M}_{\rm acc}$ is the mass accretion rate and $\upsilon_{\perp}$ is the inward component of the stream's velocity at the impact with the outer disc edge. Equation (2) indicates that when the mass accretion rate increases, the luminosity of the hot spot must also increase. In addition, our results (Section 5.3) indicate that when the mass accretion rate increases, the radius of the bright spot (if it is the source of flickering) also increases, while its temperature remains almost constant. In this case, the quasi-periods (Section 6.1) are not connected with the Keplerian rotation but probably with fragmentation and/or variability in the stream.

6.3 Temperature in the accretion disc

The time-scales of changes of the overall structure of the accretion disc (e.g. the mass transfer rate, angular momentum transport, global spiral structure formation) are longer compared with the local fluctuating processes in the flow that are responsible for the flickering activity. In this way, the dynamical time-scale variability of the flickering light source does not change the overall structure of the accretion disc. Considering the entire disc structure, the temperature in the disc can be approximated by the radial temperature profile of a steady-state accretion disc (e.g. Frank, King & Raine 2002):

$$T_{\rm eff}^4 = \frac{3 G \dot{M}_{\rm acc} M_{\rm WD}}{8 \pi \sigma R^3} \left[1 - \left(\frac{R_{\rm WD}}{R} \right)^{1/2} \right], \quad (3)$$

where R is the radial distance from the white dwarf. We assume $M_{\rm WD} = 1.35$ $M_{\odot}$. In the standard model, a white dwarf with mass 1.2–1.4 $M_{\odot}$ is expected to have a radius of 0.006–0.002 $R_{\odot}$ (e.g. Magano, Vilas Boas & Martins 2017). The average mass accretion rate in quiescence is about 2.3×10^{-7} $M_{\odot}$ yr^{-1} (Skopal 2015b). The variability of the hot component in the B band (see Fig. 5b) implies that the mass accretion rate in quiescence varies approximately from 1×10^{-7} to 5.5×10^{-7} $M_{\odot}$ yr^{-1}.

Using the parameters for RS Oph, a temperature of $7500 \le T_{\rm fl} \le$ 14 500 K (the temperature of the flickering light source as derived in Section 5.2) should be achieved at a distance $R \approx 0.5-2.0$ $R_{\odot}$ from the white dwarf. If the vortexes are 1000 K hotter than their surroundings, then this distance is $R \approx 0.6-2.6$ $R_{\odot}$ from the white dwarf. These values are similar to the Keplerian radii corresponding to the quasi-periods in the flickering light curves (see Section 6.1). If the accretion disc itself (vortexes, blobs or other structures in the disc, e.g. Bisikalo et al. 2001) is the place for the origin of the flickering of RS Oph, then the flickering comes from $R \sim 1$ $R_{\odot}$ from the WD.

6.4 X-ray emission from the boundary layer

RS Oph is an X-ray-faint recurrent nova. The X-ray observations point to a 'missing boundary layer' (Mukai 2008). However, the flickering source of RS Oph is considerably brighter in the visible and near-infrared (V, R and I bands) than the flickering source of T CrB, which is an X-ray-bright source (Mukai et al. 2013). For example, in the R and I bands, RS Oph has flickering with an amplitude larger than 0.20 mag, while in T CrB the flickering in the R and I bands has an amplitude less than 0.03 mag. In the V band, RS Oph has flickering with an amplitude larger than 0.30 mag, while for T CrB it is ≤ 0.05 mag (e.g. Zamanov et al. 2010, 2016).

If the boundary layer is completely optically thick, this could explain why RS Oph is X-ray-faint. In this case, the radius of the flickering source measured in the optical bands (Fig. 8) could represent the radius up to which the hard X-rays generated from the boundary layer are effectively processed by the inner parts of the accretion disc and the accretion disc corona.

7 CONCLUSIONS

We have reported our observations of the flickering variability of the recurrent nova RS Oph, simultaneously in the B and V bands. We estimate an interstellar reddening towards RS Oph of $E(B-V) = 0.69 \pm 0.07$ and a spectral type for the giant of M2III. Subtracting the red giant contribution, we find that the dereddened colour $(B-V)_0$ of the hot component changes from –0.4 to 0.3 and becomes redder when it becomes brighter.

For the flickering light source in RS Oph, we estimate an average $(B-V)_0 = 0.18 \pm 0.12$ and $T_{\rm fl} = 9800 \pm 2400$ K, which is similar to the temperature of the bright spot in cataclysmic variables. Its average radius is $R_{\rm fl} = 3.6 \pm 1.4$ $R_{\odot}$, and the average luminosity is $L_{\rm fl} = 89 \pm 35$ $L_{\odot}$. When the brightness of the hot component increases, the temperature of flickering source remains approximately constant and the radius of the flickering source increases.

If the flickering of RS Oph is coming from a bright spot, our results indicate that when the brightness increases the size of the spot also increases. If the flickering comes from the accretion disc, it is probably generated at a distance of ~ 1 $R_{\odot}$ from the white dwarf.

In any case, the richness of the photometric behaviour reported in this paper represents a challenging data set for further theoretical studies.

ACKNOWLEDGEMENTS

This work was partly supported by the Program for Career Development of Young Scientists, Bulgarian Academy of Sciences (DFNP 15-5/24.07.2017), by grants DN 08/1 13.12.2016, DN 12/13 12.12.2017 (Bulgarian National Science Fund), and AYA2016-76012-C3-3-P from the Spanish Ministerio de Economía y Competitividad (MINECO). We are grateful to an anonymous referee whose comments and suggestions helped to improve the original manuscript.

REFERENCES

Adamakis S., Eyres S. P. S., Sarkar A., Walsh R. W., 2011, MNRAS, 414, 2195
Ahmad I. A., Chapman R. D., Kondo Y., 1983, A&A, 126, L5
Alexander R. D., Wynn G. A., King A. R., Pringle J. E., 2011, MNRAS, 418, 2576
Anupama G. C., Mikołajewska J., 1999, A&A, 344, 177
Bagnulo S., Jehin E., Ledoux C., Cabanac R., Melo C., Gilmozzi R., ESO Paranal Science Operations Team, 2003, The Messenger, 114, 10
Baptista R., Borges B. W., Oliveira A. S., 2016, MNRAS, 463, 3799
Bessell M. S., 1979, PASP, 91, 589

Bisikalo D. V., Boyarchuk A. A., Kilpio A. A., Kuznetsov O. A., 2001, Astron. Rep., 45, 676
Bode M. F., Harman D. J., O'Brien T. J., Bond H. E., Starrfield S., Darnley M. J., Evans A., Eyres S. P. S., 2007, ApJ, 665, L63
Bode M. F., O'Brien T. J., Osborne J. P. et al., 2006, ApJ, 652, 629
Bonev T., Dimitrov D., 2010, Bulg. Astron. J., 13, 153
Booth R. A., Mohamed S., Podsiadlowski P., 2016, MNRAS, 457, 822
Brandi E., Quiroga C., Mikołajewska J., Ferrer O. E., García L. G., 2009, A&A, 497, 815
Bruch A., 1980, Inform. Bull. Variable Stars, 1805, 1
Bruch A., 1992, A&A, 266, 237
Bruch A., Duschl W. J., 1993, A&A, 275, 219
Copperwheat C. M., Marsh T. R., Dhillon V. S., Littlefair S. P., Hickman R., Gänsicke B. T., Southworth J., 2010, MNRAS, 402, 1824
Dobrzycka D., Kenyon S. J., 1994, AJ, 108, 2259
Dobrzycka D., Kenyon S. J., Milone A. A. E., 1996, AJ, 111, 414
Elsworth Y. P., James J. F., 1982, MNRAS, 198, 889
Evans A., Bode M. F., O'Brien T. J., Darnley M. J., 2008, in Evans A., Bode M. F., O'Brien T. J., Darnley M. J., eds, RS Ophiuchi (2006) and the Recurrent Nova Phenomenon, ASP Conference Series, 401
Fekel F. C., Joyce R. R., Hinkle K. H., Skrutskie M. F., 2000, AJ, 119, 1375
Frank J., King A., Raine D. J., 2002, Accretion Power in Astrophysics, Cambridge Univ. Press, Cambridge
Georgiev Ts., Zamanov R. K., Boeva S. et al., 2018, Bulg. Astron. J., in preparation
Gromadzki M., Mikolajewski M., Tomov T., Bellas-Velidis I., Dapergolas A., Galan C., 2006, AcA , 56, 97
Henden A., Munari U., 2006, A&A, 458, 339
Houdashelt M. L., Bell R. A., Sweigart A. V., Wing R. F., 2000, AJ, 119, 1424
Jackson J. C., 1975, MNRAS, 172, 483
King A. R., Pringle J. E., 2009, MNRAS, 397, L51
Kundra E., Hric L., 2014, Contrib. Astron. Obs. Skalnate Pleso, 43, 459
Kundra E., Hric L., Gális R., 2010, in Prša A., Zejda M., eds, Binaries - Key to Comprehension of the Universe, ASP Conference Series, 435, 341
Lyubarskii Y. E., 1997, MNRAS, 292, 679
Magano D. M. N., Vilas Boas J. M. A., Martins C. J. A. P., 2017, Phys. Rev. D, 96, 083012
Marsh T. R., 1988, MNRAS, 231, 1117
Martí J., Luque-Escamilla P. L., García-Hernández M. T., 2017, Bulg. Astron. J., 26, 91
Mikołajewska J., Shara M. M., 2017, ApJ, 847, 99
Mondal A., Anupama G. C., Kamath U. S., Das R., Selvakumar G., Mondal S., 2018, MNRAS, 474, 4211
Mukai K., 2008, in Evans A., Bode M. F., O'Brien T. J., Darnley M. J., eds. RS Ophiuchi (2006) and the Recurrent Nova Phenomenon ASP Conference Series., 401,p. 84.
Mukai K., Sokoloski J. L., Nelson T., Luna G. J. M., 2013, Binary Paths to Type Ia Supernovae Explosions, Proceedings of the International Astronomical Union, IAU Symposium 281, 186
Munari U., Zwitter T., 1997, A&A, 318, 269
Narumi H., Hirosawa K., Kanai K., Renz W., Pereira A., Nakano S., Nakamura Y., Pojmanski G., 2006, IAU Circ., 8671, 2
Nelson T., Mukai K., Orio M., Luna G. J. M., Sokoloski J. L., 2011, ApJ, 737, 7
O'Brien T. J., Bode M. F., Porcas R. W. et al., 2006, Nature, 442, 279
Popov V., Dimitrov D., 2011, Bulg. Astron. J., 15, 113
Puspitarini L., Lallement R., Chen H.-C., 2013, A&A, 555, A25
Ribeiro T., Baptista R., Harlaftis E. T., Dhillon V. S., Rutten R. G. M., 2007, A&A, 474, 213
Robinson E. L., Nather R. E., Patterson J., 1978, ApJ, 219, 168
Rodrigo C., Solano E., Bayo A. 2018, The SVO Filter Profile Service, avaible at: http://ivoa.net/documents/Notes/SVOFPS/index.html
Rupen M. P., Mioduszewski A. J., Sokoloski J. L., 2008, ApJ, 688, 559
Scaringi S., Körding E., Uttley P., Knigge C., Groot P. J., Still M., 2012, MNRAS, 421, 2854
Schaefer B. E., 2010, ApJS, 187, 275
Shenavrin V. I., Taranova O. G., Nadzhip A. E., 2011, Astron. Rep., 55, 31
Shu F. H., 1976, in Eggleton P., Mitton S., Whelan J., eds, Structure and Evolution of Close Binary Systems, IAU Symposium, 73, 253
Simon V., Hudec R., Hroch F., 2004, Inform. Bull. Variable Stars, 5562, 1
Skopal A., 2015a, New Astron., 36, 128
Skopal A., 2015b, New Astron., 36, 139
Smak J., 1971, Acta Astron., 21, 15
Snijders M. A. J., 1987, Ap&SS, 130, 243
Sokoloski J. L., Bildsten L., 2010, ApJ, 723, 1188
Sokoloski J. L., Bildsten L., Ho W. C. G., 2001, MNRAS, 326, 553
Sokoloski J. L., Luna G. J. M., Mukai K., Kenyon S. J., 2006, Nature, 442, 276
Somero A., Hakala P., Wynn G. A., 2017, MNRAS, 464, 2784
Starrfield S., 2008, in Evans A., Bode M. F., O'Brien T. J., Darnley M. J., eds. RS Ophiuchi (2006) and the Recurrent Nova Phenomenon, ASP Conference Series, 401, p. 4
Straizys V., Sudzius J., Kuriliene G., 1976, A&A, 50, 413
Strigachev A., Bachev R., 2011, Bulg. Astron. J., 16, 144
Tody D., 1993, in Astronomical Data Analysis Software and Systems II, ASP Conf.onference Series, 52:173
van Belle G. T., Lane B. F., Thompson R. R. et al., 1999, AJ, 117, 521
Vaytet N. M. H., O'Brien T. J., Page K. L., Bode M. F., Lloyd M., Beardmore A. P., 2011, ApJ, 740, 5
Walker A. R., 1977, MNRAS, 179, 587
Wood J. H., Horne K., Berriman G., Wade R. A., 1989, ApJ, 341, 974
Worters H. L., Eyres S. P. S., Bromage G. E., Osborne J. P., 2007, MNRAS, 379, 1557
Worters H. L., Rushton M. T., 2014, MNRAS, 442, 2637
Zamanov R., Boer M., Le Coroller H., Panov K., 2006, Inform. Bull. Variable Stars, 5733, 1
Zamanov R., Latev G., Boeva S. et al., 2015, MNRAS, 450, 3958
Zamanov R., Semkov E., Stoyanov K., Tomov T., 2016, Astron. Telegram, 8675
Zamanov R. K., Boeva S., Bachev R. et al., 2010, MNRAS, 404, 381
Zamanov R. K., Latev G. Y., Boeva S., Ibryamov S., Nikolov G. B., Stoyanov K. A., 2017, Astron. Nach., 338, 598
Zhang E.-H., Robinson E. L., 1987, ApJ, 321, 813
Zhong J., Lépine S., Li J. et al., 2015, RAA, 15, 1154

This paper has been typeset from a TEX/LATEX file prepared by the author.